

Effect of Airflow Rate Blown from a Contact Surface on Break Arcs Occurring in a 100VDC/5A Resistive Circuit

Naoki KANDA^{†a)}, *Student Member* and Junya SEKIKAWA^{†b)}, *Member*

SUMMARY In a 100VDC/5A resistive circuit, silver electrical contacts with airflow ejection structure are separated at a constant speed. Break arcs are generated between the contacts and blown by the airflow between the contact gap. Airflow rate is varied by changing shapes of the contacts. The break arcs are observed by two high-speed cameras. Following results are shown. Arc duration is shortened by the airflow. When the airflow rate is increased, the arc duration becomes shorter, and the break arcs are driven farther outward from the center axis of the contacts and are extinguished in a shorter length.

key words: break arc, electrical contacts, high-speed camera, relay

1. Introduction

When DC circuits are interrupted by electrical contacts, occurrence of break arcs is inevitable. If high-temperature break arcs continue during the contact separating, not only the electrical contacts but also the surrounding structures are damaged. Therefore, it is necessary to quickly and surely extinguish break arcs. Therefore, characteristics of break arcs are studied by many researchers [1]–[6]. One of the effective methods for arc extinction is a magnetic blowing-out [5], [6]. The authors also have investigated the characteristics of break arcs magnetically blown-out [7]–[14].

As an arc extinguishing method different from magnetic blowing out, the authors have proposed a new method to extinguish break arcs by airflow ejected from contact surface [15]. The airflow is ejected into the contact gap from the center of the surface of a movable contact with its separating motion. The airflow is generated only by the separating motion, is ejected from a hole on the center axis of the movable contact and flows radially outward in the contact gap.

The purpose of this paper is to investigate the effect of the above-mentioned airflow to break arcs and confirm the shortening effect of arc duration. Airflow rate is varied by changing shapes of movable contacts. The break arcs are generated in a 100VDC/5A resistive circuit.

2. Experimental Methods

Figure 1 shows an experimental circuit. The circuit consists of a DC power supply E , a switch, a load resistor R_1 , a pair

of electrical contacts, and a current-measuring resistor R_2 . These resistors are metal clad resistors with non-inductive windings. The R_2 is $1\ \Omega$. The E is 100 V. The circuit current when the contacts and the switch are closed is defined as I_0 . The I_0 is 5 A. The cathode is fixed, and the anode is movable. The opening speed v of the movable anode is 1.0 m/s. High-speed cameras are used to observe break arcs from two directions as shown in Fig. 2. The side and top cameras take images of the break arcs generated between the contacts from horizontally and vertically, respectively. The frame rate of high-speed cameras is 10000 frames per second and the exposure time is $97\ \mu\text{s}$.

Types of contact shapes are listed in Table 1. The diameter of fixed cylinders D_f is different for each type.

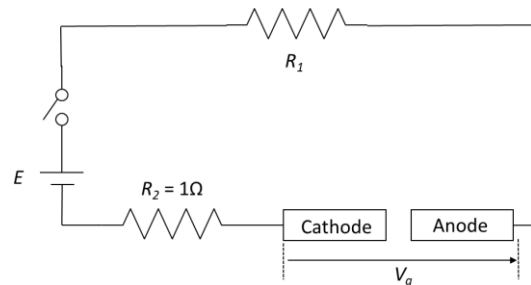


Fig. 1 Experimental circuit.

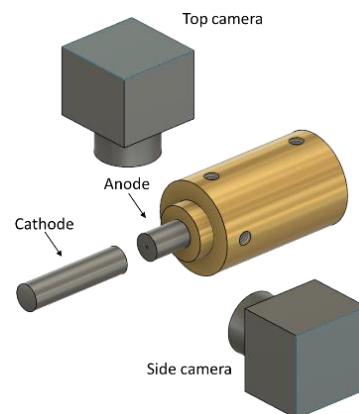


Fig. 2 Arrangement of electrical contacts and high-speed cameras.

Table 1 Types of contact shapes.

Type	Diameter of fixed cylinder D_f [mm]
1	4
2	8

Manuscript received January 10, 2024.

Manuscript revised July 25, 2024.

Manuscript publicized August 29, 2024.

[†]Graduate School of Engineering, Shizuoka University, Hamamatsu-shi, 432–8561 Japan.

a) E-mail: kanda.naoki.19@shizuoka.ac.jp

b) E-mail: sekikawa.junya@shizuoka.ac.jp

DOI: 10.1587/transle.2024EMS0002

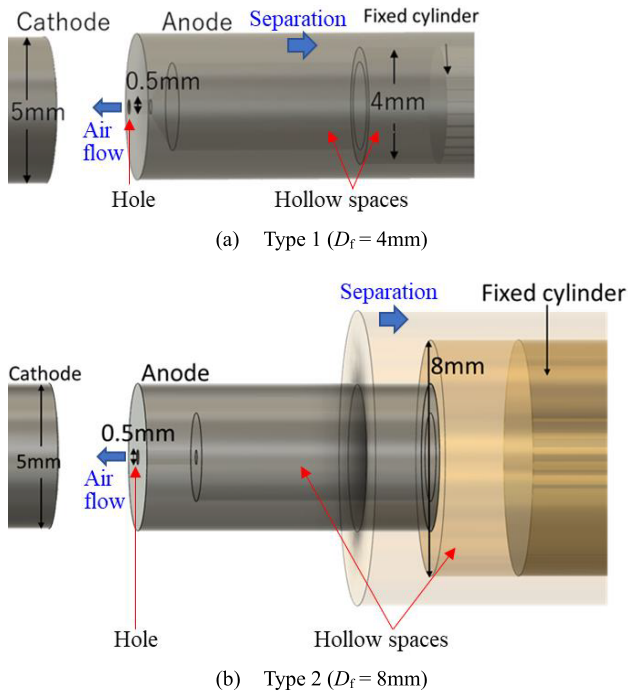


Fig. 3 Contact shapes.

Contact shapes of the electrical contacts for each type are shown in Fig. 3. As an example, a structure of the anode and the air flow from the anode is explained for the type 1 shown in Fig. 3 (a). There is a fixed cylinder in a hollow space in the anode. During contact separation, the fixed cylinder does not move, and only the anode moves. Air in the hollow space is ejected from the hole when the anode is separated. Therefore, airflow from the hole to contact gap is generated during contact separating. The airflow ejected from the hole on the anode expands radially in the contact gap. This airflow is expected to move break arcs outside the contact gap during contact separating. For type 2, the diameters of a fixed cylinder and a hollow part are increased to 8 mm to increase airflow rate as shown in Fig. 3 (b). In the case of Type 2 compared to Type 1, the diameter of the fixed cylinder is twice as large and its cross-sectional area is four times as large, so the amount of air ejected from the hole is expected to be four times as large.

The contacts are made of pure silver (99.99%). The cathode is cylindrical with a diameter of 5 mm and its surfaces is slightly curved. In order to compare the results with and without airflow, for each type without airflow, the fixed cylinder is removed, and experiments are carried out. Five break operations are performed for each experimental condition.

3. Experimental Results

Typical experimental results for each type are shown in Figs. 4 and 5. These results are typical examples when the arc duration is closest to the average value for each experimental condition.

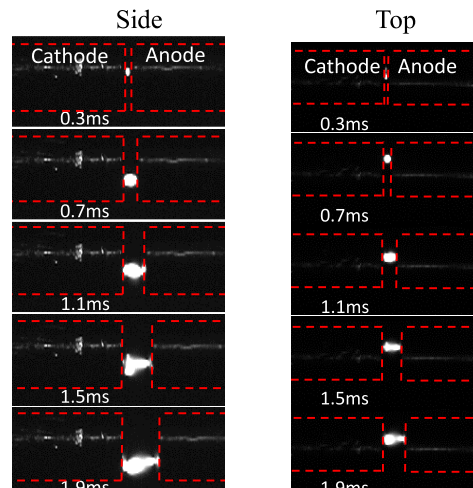
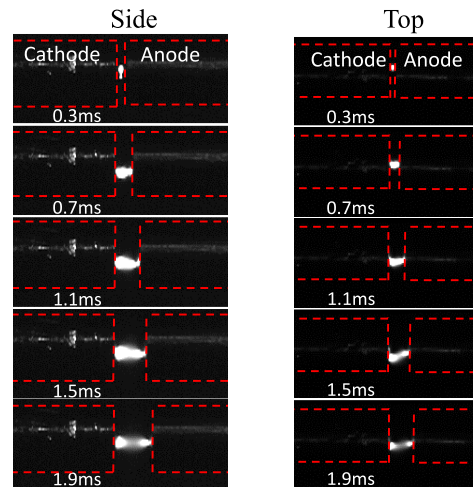
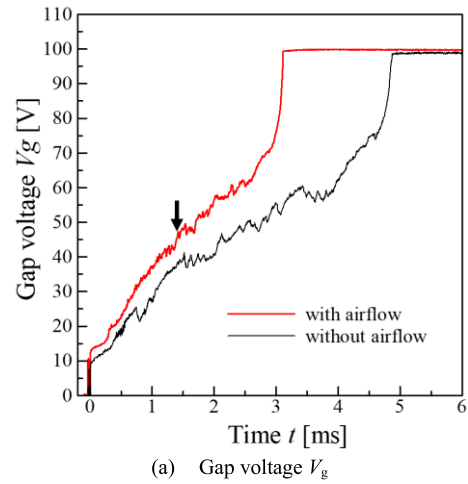


Fig. 4 Typical break arcs (Type 1).

For the cases with and without airflow for the type 1, as shown in Fig. 4 (a), the V_g increased almost the same rate until about 1.4 ms, after that, the V_g with airflow increased slightly more quickly than that without airflow. Figures 4 (b) and 4 (c)

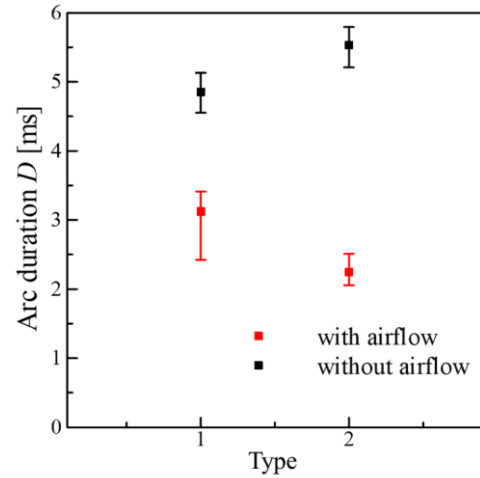
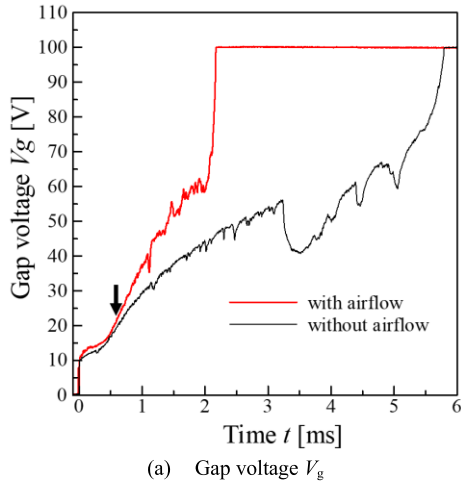


Fig. 6 Arc duration.

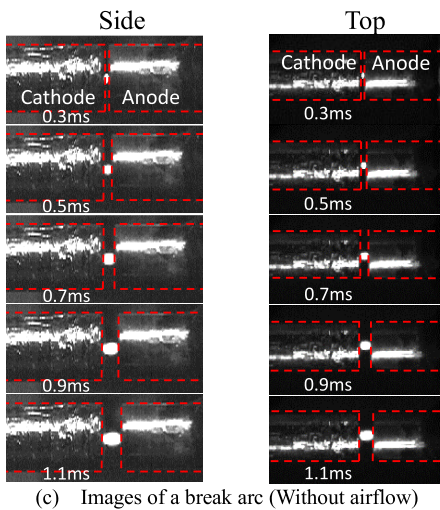
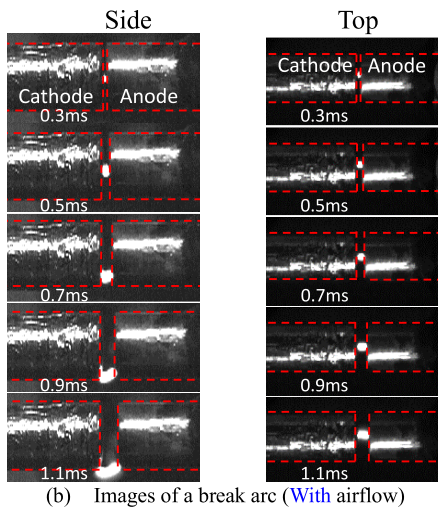


Fig. 5 Typical break arcs (Type 2).

indicate images of the break arcs observed by the high-speed cameras with and without airflow, respectively. The break arc almost stays near the central axis of the contacts without airflow as shown in Fig. 4 (c). In contrast, with airflow, the break arc moves gradually outward from the central axis of

the contacts from 1.1 ms to 1.9 ms as shown in “Top” images of Fig. 4 (b), but the motion is not so significant.

As shown in Fig. 5 (a), with and without airflow for the type 2, the time evolutions of the V_g are almost identical until about 0.6 ms, after that, the V_g increases more quickly in the case with airflow until arc extinction. Figures 5 (b) and 5 (c) represent images of the break arcs with and without airflow for the type 2, respectively. As shown in Fig. 5 (c), “Side” images show that the break arc stays almost near the central axis of the contacts without airflow. With airflow, in contrast, the break arc moves gradually outward from the central axis of the contacts from 0.5 ms as shown in “Side” images of Fig. 5 (b).

The results for the types 1 and 2 with airflow are compared. As shown by arrows in Figs. 4 (a) and 5 (a), the timing of the V_g increasing is earlier for the type 2 than that for the type 1. Comparing motion of the break arcs, the break arc for the type 2 is driven further to the outside than that for the type 1 as shown in Figs. 4 (b) and 5 (b).

Arc duration D for each experimental condition is shown in Fig. 6. With airflow, the D for the type 2 is shorter than that for the type 1.

These results shown above indicate that the break arcs are driven more strongly, and the arc duration is shorter when the airflow rate is increased, because the airflow rate for the type 2 is higher than that for the type 1 with airflow.

4. Discussion

As shown in previous chapter, the break arcs were driven, and the arc duration was shortened by the airflow. There are two possible reasons for these results. One of them is the effect of lengthening the break arcs due to the airflow, and the other is the cooling effect by the airflow.

Figure 7 shows images of the break arcs just before arc extinction. With airflow, as shown in Fig. 7 (a), the break arc for the type 1 is slightly lengthened diagonally in the contact gap. On the other hand, the break arc for the type 2 is lengthened outer than the contact gap and deformed into

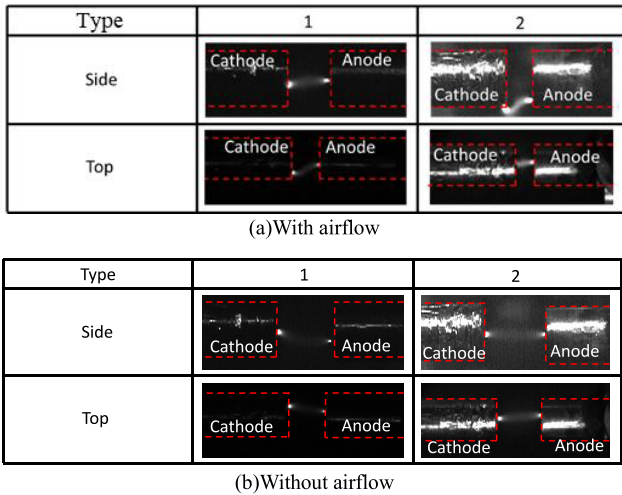


Fig. 7 Break arcs just before arc extinction with and without airflow.

Table 2 Arc length just before arc extinction with airflow.

Type	Arc Length [mm]
1	3.8
2	2.5

more complex shape.

As shown in Fig. 7 (b), without airflow, the shape of the break arc for the type 1 is slightly diagonal to the central axes of the contacts. This shape is due to the random motion of the break arc during the arc duration. For the type 2, the shape of the break arc is almost straight because the break arc almost stayed in the contact gap.

Table 2 shows the arc length just before arc extinction for the types 1 and 2 with airflow. These lengths were analyzed three-dimensionally considering arc deformation. The length just before arc extinction for the type 2 is shorter than that for the type 1. Therefore, the shortening of the arc duration will be obtained not only due to the arc lengthening effect, but also to the cooling effect by higher airflow rate, which leads to the arc extinction with shorter arc length.

For the break arcs between the contacts without airflow, the break arcs tended to move slightly randomly for the type 1, and they tended almost to stay for the type 2. However, in the cases with airflow, in both Type 1 and Type 2, the break arcs were driven in a certain direction by the airflow, without random motion or staying. Therefore, in the case with airflow for the type 2, it is clear that the break arcs were driven and surrounded by the airflow, and there is no contradiction that they were cooled by the airflow.

5. Conclusion

In the 100VDC/5A resistive circuit, silver electrical contacts with airflow ejection structure were separated at the constant speed. Break arcs were generated between the contacts and blown by the airflow between the contact gap. The airflow rate was varied by changing shapes of the contacts. Follow-

ing results were obtained.

- (1) Arc duration was shortened by the airflow.
- (2) When the airflow rate was increased, the arc duration became shorter, and the break arcs were driven farther outward from the center axis of the contacts and were extinguished in a shorter length.

References

- [1] M. Hasegawa, "Influences of contact opening speeds on break arc behaviors of AgSnO_2 contact pairs in DC inductive load conditions," *IEICE Trans. Electron.*, vol.E98-C, no.9, pp.923–927, Sept. 2015.
- [2] J. Wei, L. Zhang, Z. Li, D. Zhang, X. Bai, M. Hasegawa, and Q. Zhu, "Effect of surrounding atmospheres on break arc durations of electrical contacts in DC load conditions," *IEICE Trans. Electron.*, vol.E103-C, no.1, pp.16–27, Jan. 2020.
- [3] X. Zhou, M. Chen, and G. Zhai, "Comparisons on arc behavior and contact performance between Cu and Cu-Mo alloys in a bridge-type contact system," *IEICE Trans. Electron.*, vol.E98-C, no.9, pp.904–911, Sept. 2015.
- [4] C. Li, Z.B. Li, Q. Wang, D. Liu, M. Hasegawa, and L. Li, "Experimental study on arc duration under different atmospheres," *IEICE Trans. Electron.*, vol.E97-C, no.9, pp.843–849, Sept. 2014.
- [5] K. Sawa, M. Tsuruoka, and M. Morii, "Fundamental characteristics of arc extinction at DC low current interruption with high voltage (<500 V)," *IEICE Trans. Electron.*, vol.E99-C, no.9, pp.1016–1022, Sept. 2016.
- [6] S. Tokumitsu and M. Hasegawa, "Relationships between break arc behaviors of AgSnO_2 contacts and Lorentz force to be applied by an external magnetic force in a DC inductive load circuit up to 20V-17A," *IEICE Trans. Electron.*, vol.E102-C, no.9, pp.641–645, Sept. 2019.
- [7] J. Sekikawa and T. Kubono, "Observation of breaking arcs of Ag or Cu electrical contact pairs with a high-speed camera," *IEICE Trans. Electron.*, vol.E87-C, no.8, pp.1342–1347, Aug. 2004.
- [8] J. Sekikawa and T. Kubono, "An experimental equation of V-I characteristics of breaking arc for Ag, Au, Cu and Ni electrical contacts," *IEICE Trans. Electron.*, vol.E86-C, no.6, pp.926–931, June 2003.
- [9] Y. Nakamura, J. Sekikawa, and T. Kubono, "Dependence of motion of breaking arc on contact separating speed for Ag and Pd contact pairs in a DC42V resistive circuit," *IEICE Trans. Electron.*, vol.E90-C, no.7, pp.1361–1368, July 2007.
- [10] H. Ono and J. Sekikawa, "Arc length of break arcs magnetically blown-out at arc extinction in a DC450V/10A resistive circuit," *IEICE Trans. Electron.*, vol.E96-C, no.9, pp.1132–1137, Sept. 2013.
- [11] K. Kato and J. Sekikawa, "Restriction on motion of break arcs magnetically blown-out by surrounding walls in a 450VDC/10A resistive circuit," *IEICE Trans. Electron.*, vol.E99-C, no.9, pp.1009–1015, Sept. 2016.
- [12] A. Ishihara and J. Sekikawa, "Arc duration and dwell time of break arcs magnetically blown-out in nitrogen or air in a 450VDC/10A resistive circuit," *IEICE Trans. Electron.*, vol.E101-C, no.9, pp.699–702, Sept. 2018.
- [13] Y. Kaneko and J. Sekikawa, "Arc length just before extinction of break arcs magnetically blown-out by an appropriately placed permanent magnet in a 200V-500VDC/10A resistive circuit," *IEICE Trans. Electron.*, vol.E103-C, no.12, pp.698–704, Dec. 2020.
- [14] H. Miyagawa and J. Sekikawa, "Effect of magnetic blow-out and air flow on break arcs occurring between silver electrical contacts with copper runners," *IEICE Trans. Electron.*, vol.E100-C, no.9, pp.709–715, Sept. 2017.
- [15] S. Hattori and J. Sekikawa, "An experimental study on effect of airflow ejected from inside of an electrical contact on break arcs," *Proc. 2022 IEICE General Conference, Electron.*, vol.2, C-5-1, p.1, March 2022.